CALAMITY
Calamity: A Journal of Disaster Technology and Engineering
CALAMITY 4(1): 1–23
ISSN 3025-4140

Institute for Advanced Science, Social and Sustainable Future
MORALITY BEFORE KNOWLEDGE

Composite tidal flood risk assessment for adaptation prioritization

Aswin Kurnia Ramadhan[1], Wezia Berkademi[1,*], Rachmadhi Purwana[1]
[1] *Department of Environmental, Graduate School of Sustainable Development, Universitas Indonesia, Central Jakarta, Special Capital Region of Jakarta 10440, Indonesia.*
*Correspondence: wezia.b@ui.ac.id

Received Date: May 11, 2026 Revised Date: June 17, 2026 Accepted Date: July 20, 2026

ABSTRACT
Background: Coastal areas of Jakarta, Indonesia face increasing flood risk due to sea-level rise, land subsidence, tidal inundation, dense urban development, and uneven social vulnerability. Existing coastal flood studies in Indonesia often analyze hazard, exposure, or vulnerability in isolation, limiting their value for integrated adaptation, especially in data-limited planning. This study aims to create a data-minimal risk assessment framework for Penjaringan District, North Jakarta, by integrating tidal flood trends, asset exposure values, and social vulnerability at the urban village level. **Methods:** The study used official tidal flood records, spatial building data, asset values from official unit costs and content ratios, and social vulnerability indicators (population density, slum settlement proportion, and malnutrition prevalence). Analysis included trend assessment, exposure estimation, min-max normalization, composite risk indexing, sensitivity analysis, risk typology, and hazard-vulnerability quadrant analysis. **Findings:** Results show a spatial mismatch between hazard concentration and composite risk. Pluit accounted for 149 of 171 flood-affected days (87.1%) and scored the highest Hazard Index (HI = 1.000), but Penjaringan reached the highest Risk Index (RI = 0.628), due to a Very High Exposure Index (EI = 0.816) and High Social Vulnerability Index (SVI = 0.667). District replacement asset value was estimated at Rp 159.42 trillion. Sensitivity analysis showed Penjaringan remained the highest risk in most scenarios, except for hazard-dominant, where Pluit ranked highest. **Conclusion:** Flood risk in Penjaringan cannot be explained by hazard frequency alone. The proposed framework offers an initial risk assessment and adaptation prioritization tool in data-limited coastal urban areas. **Novelty/Originality:** This study presents a replicable framework combining tidal flood records, asset exposure values, social vulnerability, composite risk indexing, sensitivity tests, risk typology, and hazard-vulnerability quadrant analysis.

KEYWORDS: coastal flood risk; composite risk index; exposure assessment; sensitivity analysis; social vulnerability.

1. Introduction

Global warming increases risks in coastal areas through rising sea levels caused by thermal expansion and melting polar ice (Nurhidayah et al., 2022). The sea level is projected to rise between 0.28–0.55 meters (low emission scenario, SSP1-1.9) and 0.63–1.01 meters (high emission scenario, SSP5-8.5), relative to the period 1995–2014 (IPCC, 2023a). The wide range of projections demonstrates that predicting a single future scenario with certainty is difficult (Siegert & Pearson, 2021).

This condition puts approximately 11% of the global population (896 million people) living in coastal areas at risk (IPCC, 2023b). Most coastal areas will experience rising sea levels (Jevrejeva et al., 2016). The combination of rising sea levels and population

Cite This Article:
Ramadhan, A. K., Berkademi, W., Purwana, R. (2026). Composite tidal flood risk assessment for adaptation prioritization. *Calamity: A Journal of Disaster Technology and Engineering, 4*(1), 1-23. https://doi.org/10.61511/calamity.v4i1.2026.3759

concentration significantly increases risks to human safety, infrastructure sustainability, and socio-economic resilience (Causevic et al., 2021). Rising sea levels further increase flood frequency, even under non-extreme conditions, where tidal flooding contributes to significant cumulative property damage (Mita et al., 2023). This global risk is amplified at the local level, particularly in coastal areas that face additional threats from land subsidence (Asmadin et al., 2021). DKI Jakarta, as one of the megacities in coastal areas, faces the impacts of rising sea levels and experiences one of the world's fastest rates of land subsidence. In the past three decades, DKI Jakarta has experienced recurring coastal flooding, with the main triggers being tides, sea level rise, wind, and land subsidence (Yusuf et al., 2025). North Jakarta has a total disaster risk index of 68.89, which is categorized as Moderate. Although it is generally at moderate risk, this area faces a High threat specific to the coastal sector, namely Flooding (score 19.02) and Extreme Waves and Erosion (score 12.68) (BNPB, 2025). The high hydrometeorological risk is also driven by the dominant Extreme Weather index score of 87.60, highlighting the urgency of prioritizing coastal disaster adaptation in this region (BNPB, 2025).

The subsidence rate in Jakarta varies between 1–10 cm/year, and it reaches 20–28 cm/year in certain hotspot areas, such as Penjaringan District, due to excessive groundwater extraction and massive urbanization (Hasibuan et al., 2023). Recent data from the 2015–2022 period show that the land subsidence rate in North Jakarta is 8.47 cm/year (Harintaka et al., 2024). Furthermore, satellite data indicate that sea levels in Jakarta rise at a rate of 3.2–4.0 mm/year, which is higher than the global average (Bott et al., 2021). When these two threats, land subsidence and sea level rise are combined, the relative sea level rise in Jakarta, especially in Penjaringan District, becomes significantly higher (Hasibuan et al., 2025). This not only intensifies the physical risks but also creates a resource allocation crisis for local governments with limited budgets. The interaction between accelerated land subsidence and sea-level rise substantially increases the frequency, depth, and spatial extent of tidal flooding, because subsidence lowers the land surface relative to the rising sea, so that relative sea-level rise exceeds the contribution of either process alone.

Flood risk should be understood as the interaction between hazard, exposure, and vulnerability, because these three dimensions jointly determine how flood events translate into tangible impacts on people, assets, and urban systems (Begum et al., 2023; Reisinger et al., 2020). Exposure refers to the presence of people, built assets, infrastructure, and economic activities in coastal flooding-affected areas. This dimension is particularly important in urban coastal environments because the concentration of residential areas, transport networks, commercial facilities, and public infrastructure can substantially increase the scale of potential disruption and loss, even under moderate inundation conditions (Pradana et al., 2023; Setiadi et al., 2020). Therefore, previous flood risk studies have emphasized the need to assess not only where hazards occur but also which assets are located in flood-prone areas and how their spatial concentration shapes the severity of potential impacts (Eaves et al., 2023; FathiAzar, 2025). Incorporating exposure into coastal flood analysis is essential for identifying the physical and economic elements at risk and for supporting more spatially targeted adaptation planning (Acosta-Morel et al., 2021; Warren-Myers & Cradduck, 2023).

Social vulnerability also shapes risk, which reflects the susceptibility of individuals or communities to harm and their limited capacity to anticipate, cope with, and recover from hazardous events (Flanagan et al., 2011). Social vulnerability is commonly associated with demographic, socioeconomic, and settlement-related conditions, including population pressure, informal housing, health status, and unequal access to resources and public services. although comprehensive frameworks incorporate various such dimensions, their operationalization in data-limited urban contexts is constrained by the availability of sub-district administrative data. Therefore, in this study, social vulnerability is represented through three indicators: population density, slum settlement proportion, and malnutrition prevalence, selected on the basis of their theoretical relevance to flood coping capacity and their availability at the urban village level.

In coastal settings, these factors often explain why similar magnitude flood events can produce unequal consequences across places and social groups (Solecki & Friedman, 2021). Therefor adaptation planning should not be based solely on where flooding occurs or which assets are exposed, but also on which communities face the greatest constraints in responding to and recovering from flood impacts (Paranunzio et al., 2022). Similar magnitude flood events for developing adaptation priorities that are not only technically effective but also socially equitable (Johnson et al., 2023; Turner et al., 2025). In Indonesian coastal contexts, social vulnerability assessments have employed composite indexing approaches that combine socio-demographic and built-environment indicators at the sub-district level (Kim & Gim, 2020; Putiamini et al., 2023). At the regional scale, composite flood risk assessment frameworks integrating hazard, exposure, and vulnerability dimensions have been applied across Southeast Asian coastal contexts, from regional-scale multi-country indices to urban village-level assessments in Indonesian coastal cities affected by land subsidence and sea-level rise (An et al., 2020; Anindita et al., 2020).

In Indonesia, particularly in coastal areas such as Jakarta, there is a gap in research integrating the three dimensions of flood risk (hazard, exposure, and vulnerability) into a comprehensive coastal flood risk assessment. Previous studies in Indonesia have examined coastal flooding from different perspectives, but focused only on physical hazards or vulnerability separately, without integrating hazard, exposure, and social vulnerability into a single assessment framework. Studies in Pekalongan and Indramayu have mainly focused on tidal inundation, sea level rise, land subsidence, and physical coastal vulnerability (Nashrrullah et al., 2013; Putiamini et al., 2023). Meanwhile, research on the northern coast of Java and Kalibaru, North Jakarta, addressed exposure, potential losses, and settlement vulnerability, but did not fully integrate historical flood trends, asset exposure, and social vulnerability into a composite coastal flood risk framework (Mutia Gunandar et al., 2024; Suroso & Firman, 2018). Unlike these studies, the proposed framework integrates historical hazard records, asset exposure valuation, and social vulnerability into a single sensitivity-tested composite index for adaptation prioritization.

This creates a methodological gap because the interaction between physical hazard, economic exposure, and the social capacity of affected communities shapes actual flood risk. The originality of this study lies in the simultaneous integration of three explicitly parameterized indices; a Hazard Index (HI) constructed from historical tidal flood frequency records, an Exposure Index (EI) derived from spatially referenced replacement asset values of classified building stocks, and a Social Vulnerability Index (SVI) operationalized through population density, slum settlement proportion, and malnutrition prevalence. These three indices are embedded within a sensitivity-tested composite Risk Index and a hazard-vulnerability quadrant analysis, forming a replicable, data-limited computational framework for adaptation prioritization in urban coastal districts with constrained planning data. Therefore, this study aims to assess coastal flood risk in Penjaringan District by identifying tidal flood trends, estimating exposed asset values, measuring social vulnerability, and prioritizing adaptation by classifying urban village-level risk profiles. This study assumes that urban villages with higher tidal flood frequency, greater exposed asset value, and higher social vulnerability will have higher composite flood risk and should therefore receive greater priority in coastal adaptation planning.

2. Methods

The Penjaringan District is located along the northern coastal edge of North Jakarta and comprise five urban villages: Penjaringan, Pluit, Pejagalan, Kapuk Muara, and Kamal Muara. The district covers 35.47 km^2 of administrative area and is positioned at the mouth of Teluk Jakarta, with elevations largely at or below mean sea level. The combination of rapid land subsidence, tidal forcing, and dense urban development creates near-permanent flood risk conditions for its estimated 288,000 residents. Tidal flood data near-permanent flood risk conditions for the form of official daily situation report spreadsheets (*Rekap Data Banjir*). Records were filtered for Penjaringan District, deduplicated so that multiple snapshots from the same calendar day and urban village counted as one flood-affected day, and processed to extract inundation depth and stated flood cause. Temporal trends were assessed using the OLS linear regression and the Mann-Kendall non-parametric test with Sen's slope (Hussain & Mahmud, 2019).

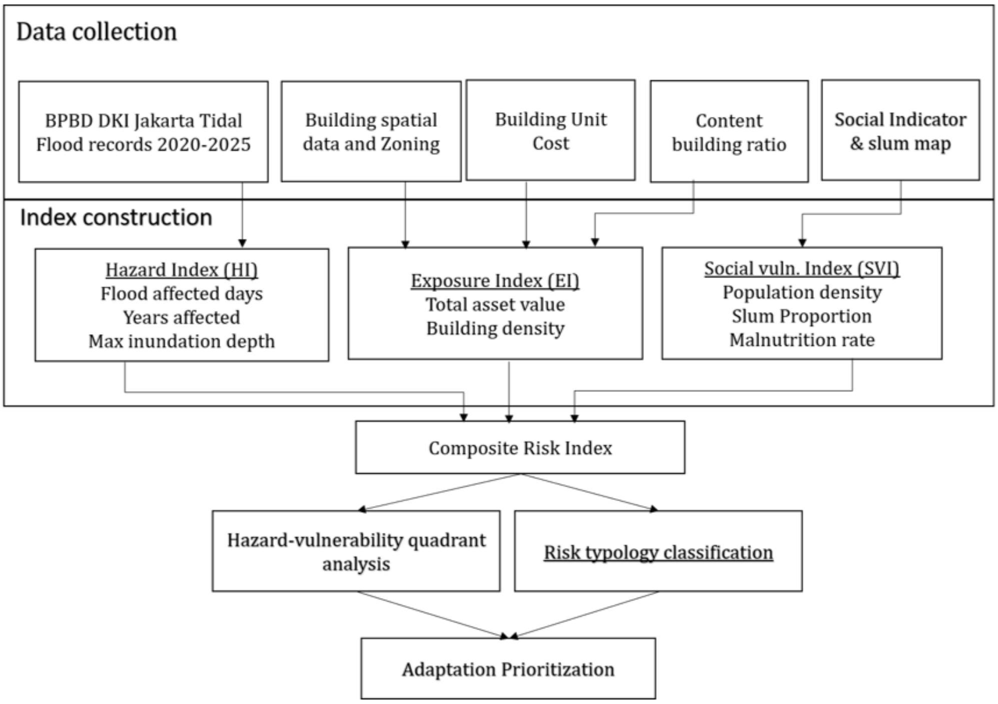

Fig. 1. Research workflow for the composite coastal flood risk assessment framework

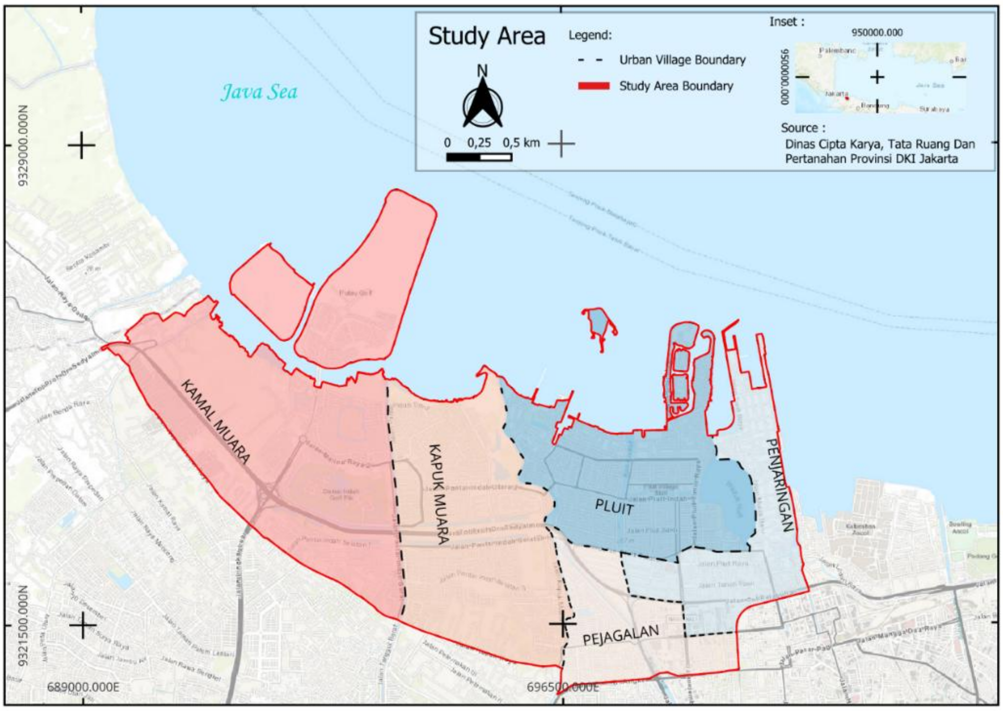

Fig. 2. Location map of Penjaringan District, North Jakarta, showing its five constituent urban villages

Building inventory data were compiled by integrating the 1:1,000 scale building polygon layer from DCKTRP (2020) with OpenStreetMap footprints, yielding 65,496 building polygons reprojected to UTM Zone 48S (EPSG:32748). Buildings were classified using centroid-based spatial join against the RDTR zoning layer, with 30 original zone categories aggregated into seven classifications. Green Space, Water Body, and Road Right-of-Way zones were exclude, leaving four active land-use classifications as the basis for exposure assessment. Building footprint area was used as the exposure unit following the Global Flood Depth-Damage method (Huizinga et al., 2017), representing a conservative lower-bound estimate of the exposed floor area. This assumption may underestimate exposure for multi-storey buildings and should therefore be interpreted as a conservative estimate. This approach is justified on two grounds: first, total floor area data by building are not available in the DCKTRP building polygon dataset; second, tidal flooding in Penjaringan is predominantly shallow (mean depth 15–34 cm across kelurahan), primarily affecting ground-floor spaces, such that footprint area provides a reasonable proxy for flood-exposed area under observed inundation conditions.

Table 1. Aggregation of RDTR zone categories into research land-use classifications

No	Classification	RDTR Zone Categories (number of zones)
1	Residential	Very High Density Housing, High Density Housing
2	Green Space and Nature	City Park, Green Belt, Permanent Production Forest, Nature Tourism Park, Mangrove Ecosystem, Protection Forest, Limited Production Forest/Water Body, Wildlife Reserve, Neighbourhood Park, District Park, Urban Village Park, Horticulture, RT Park, Permanent Production Forest/Road Right-of-Way
3	Industrial and Infrastructure	Industrial Zone, Power Generation Facility
4	Road Right-of-Way	Road Body
5	Commercial and Services	WP-Scale Trade and Services, SWP-Scale Trade and Services, WK-Scale Trade and Services
6	Water Body	Water Body
7	Government and Public Facilities	City-Scale Public Service, Local Protection Zone, Transportation, District-Scale Public Service, Urban Village-Scale Public Service, Government Office, Defence and Security

Maximum asset values per building were assigned using unit replacement costs from the Governor of DKI Jakarta Decree No. 580/2025 (SHSBGN) combined with content-to-structure ratios from Huizinga et al. (2017, Appendix C), as summarized in Table 2. The total asset value per building was computed as $V = A \times C \times (1 + r)$, where A is the footprint area (m^2), C is the structural unit cost (IDR million/m^2), and r is the content-to-structure ratio. Buildings were assigned to Types A–E according to the footprint-area thresholds defined in Table 2, applied uniformly to all residential building polygons, with urban village-level weighted average unit costs derived from the empirical type distribution. Building density was computed as the total number of building polygons in each urban village divided by its administrative area (units/km^2), using the same building footprint dataset employed for asset valuation.

Table 2. Standard building unit prices and content ratios by land-use classification

No	Classification	Structural Cost (IDR million/m^2)	Content Ratio	Content Value (IDR million/m^2)	Total (IDR million/m^2)
1a	Residential Type A (>120 m^2)	7.56	50%	3.78	11.34
1b	Residential Type B (70–120 m^2)	7.48	50%	3.74	11.22
1c	Residential Type C (54–70 m^2)	6.23	50%	3.12	9.35
1d	Residential Type D (36–54 m^2)	5.80	50%	2.90	8.70
1e	Residential Type E (<36 m^2)	5.50	50%	2.75	8.25
2	Commercial and Services	7.73	100%	7.73	15.46
3	Industrial and Infrastructure	6.94	150%	10.41	17.35
4	Government and Public Facilities	7.73	50%	3.87	11.60

(Huizinga et al., 2017)

 https://doi.org/10.61511/calamity.v4i1.2026.3759

Social vulnerability indicators were compiled from two primary sources at the urban village level. Population density and prevalence of malnutrition were obtained from BPS Kota Jakarta Utara, *Kecamatan Penjaringan Dalam Angka* 2024. The population density was calculated as the ratio of the total population to urban village area (persons/km^2). The prevalence of malnutrition was expressed as recorded cases per 1,000 population. The proportion of slum settlement area was derived spatially through the overlay of the DKI Jakarta Slum Settlement Map (*Peta Permukiman Kumuh*, DCKTRP, 2025) against urban village administrative boundaries in QGIS, computed as the ratio of slum-classified area (ha) to total urban village area (ha). Because they capture key dimensions of social vulnerability, including demographic pressure, settlement quality, and baseline health status, while ensuring consistent data availability at the urban village level

Table 3. Sub-indicators of the hazard index (HI), exposure index (EI), and social vulnerability index (SVI)

Index	Sub-indicator	Metric	Rationale
HI	Total number of flood-affected days	Days during the observation period	Overall flood frequency during the observation period
HI	Temporal consistency	N years affected (out of 6)	Persistence and regularity of the flood hazard
HI	Maximum inundation depth	cm	Flood severity; empirical upper-bound intensity under observed conditions
EI	Total asset value	IDR Trillion	Overall magnitude of economic exposure across the four built-asset classifications
EI	Building density	Units/km^2	Intensity of built environment independent of asset value
SVI	Population density	Persons/km^2	Concentration of people exposed to flood hazard and emergency response demand
SVI	Slum settlement proportion	% of the urban village area	Structural housing inadequacy and limited adaptive capacity of the built environment
SVI	Malnutrition rate	Cases per 1,000 population	Baseline health vulnerability; reduced capacity to cope with flood stress

A multi-dimensional Risk Index (RI) was constructed by integrating three component indices: a Hazard Index (HI), an Exposure Index (EI), and a Social Vulnerability Index (SVI), each operationalized at the urban village level, following the hazard-exposure-vulnerability risk decomposition approach (UNDRR, 2015). All inputs are derived from routinely produced government administrative and spatial data without recourse to hydrodynamic simulation. Each sub-indicator was normalized to a [0, 1] scale using the following min-max transformation:

$$norm = (I - I_{min}) / (I_{max} - I_{min}) \quad \text{(Eq. 1)}$$

Where higher values indicate greater hazard, exposure, or vulnerability. Min-max normalization was applied because it rescales sub-indicators with different measurement units onto a common dimensionless [0, 1] scale while preserving their relative ordering, enabling aggregation across dimensions. Each component index was computed as the unweighted arithmetic mean of its normalized sub-indicators, and the composite Risk Index as:

$$RI = (HI + EI + SVI) / 3 \quad \text{(Eq. 2)}$$

To facilitate direct cross-dimensional comparison, all four indices were classified using uniform equal-interval thresholds (Table 4).

Table 4. Equal-interval classification thresholds applied uniformly to HI, EI, SVI, and RI

Score	Class
0.80 – 1.00	Very High
0.60 – 0.79	High
0.40 – 0.59	Moderate
0.20 – 0.39	Low
0.00 – 0.19	Very Low

The three-component indices were constructed using different sets of sub-indicators. The Hazard Index (HI) and Social Vulnerability Index (SVI) were each constructed from three sub-indicators, while the Exposure Index (EI) was constructed from two sub-indicators: total asset value and building density, as detailed in Table 3. Equal weighting was adopted because no empirical or stakeholder-derived weighting scheme was available for the study area, avoiding subjective prioritization among the three dimensions; the implications of this choice are examined through the four-scenario sensitivity analysis. Sensitivity analysis tested ranking stability under four weighting scenarios: S0 (equal weights: HI = EI = SVI = 1/3), S1 (hazard-dominant: HI = 0.50, EI = SVI = 0.25), S2 (exposure-dominant: EI = 0.50, HI = SVI = 0.25), and S3 (vulnerability-dominant: SVI = 0.50, HI = EI = 0.25), using RI = (wH × HI) + (wE × EI) + (wS × SVI).

Risk typology classification identified the dominant risk driver per urban village: Hazard-Dominant (HD) when HI was highest, Exposure-Dominant (ED) when EI was highest, Vulnerability-Dominant (VD) when SVI was highest, and Compound Risk (CR) when two or more indices simultaneously reached the High or Very High class. This criterion was adopted because concurrent high values across multiple dimensions indicate interacting risk drivers that require integrated, rather than single-sector, adaptation measures. A hazard-vulnerability quadrant analysis positioned each urban village in HI × SVI space, divided by district mean values (mean HI = 0.367; mean SVI = 0.337), into four quadrants: Q1 (High Hazard – High Vulnerability), Q2 (Low Hazard – High Vulnerability), Q3 (Low Hazard – Low Vulnerability), and Q4 (High Hazard – Low Vulnerability). The mean values were selected as quadrant boundaries because, with only five observation units, the median coincides exactly with Pejagalan's own index values, making the classification threshold sensitive and inconsistent with its component index classes.

Spatial visualization was conducted by linking the urban village-level index scores to the administrative boundary layer and mapping all four indices using equal-interval classification with consistent color ramps. This study has several methodological limitations. First, the flood observation period covers only January 2020 to September 2025, with 2025 representing only nine months, which limits the statistical power for detecting long-term trends. Second, the absence of a hydrodynamic simulation means that the exposure estimates represent the urban village-level potential exposure under full-inundation assumptions rather than event-specific inundation loss and cannot resolve spatial variation within individual urban villages. Third, the building footprint area as the exposure unit may underestimate the total floor area in multi-story structures. Fourth, the SVI only incorporates indicators available at the urban village level from published government sources; broader dimensions, including poverty rate, age dependency, educational attainment, and disability, could not be included due to data unavailability at this administrative scale. Despite these limitations, the proposed framework provides a transparent and replicable method for prioritizing coastal flood risk using routinely available administrative and spatial data.

3. Results and Discussion

3.1 Result

This section presents the results of the multi-criteria flood risk assessment for Penjaringan District, structured around the four component outputs of the analytical framework; historical tidal flood characteristics and the Hazard Index, building asset exposure and the Exposure Index, social vulnerability and the Social Vulnerability Index, and the integrated Risk Index. Results are presented at the urban village level across all five administrative sub-units of Penjaringan District.

3.1.1 Historical characteristics of tidal floods and hazard index

A total of 171 flood-affected days were recorded across Penjaringan District between January 2020 and September 2025 (Table 5). Tidal flooding was overwhelmingly concentrated in Pluit (149 days, 87.1%), with annual counts ranging from 2 days (2023) to 59 days (2024). The remaining four urban villages collectively contributed 22 days or 12.9% of the total district.

Table 5. Annual flood-affected days by urban village, Penjaringan District, 2020–2025

Urban village	2020	2021	2022	2023	2024	2025	Total	% of the Total
Pluit	18	9	14	2	57	49	149	87.1%
Penjaringan	3	2	3	0	2	0	10	5.8%
Pejagalan	3	2	0	0	0	0	5	2.9%
Kapuk Muara	5	1	0	0	0	0	6	3.5%
Kamal Muara	0	1	0	0	0	0	1	0.6%
Penjaringan District	29	15	17	2	59	49	171	100%

The OLS linear regression produced a positive district-level slope of +6.20 days/year (R^2 = 0.284). The Mann-Kendall test also showed a positive direction, with τ = +0.200 and Sen's slope = +4.00 days/year. However, neither test was statistically significant, with p-values of 0.276 and 0.707, respectively. The HI uses observed flood frequency as a descriptive measure of the historical hazard burden rather than as a trend-based projection; the non-significant trend therefore does not invalidate frequency as a hazard indicator, but indicates that the short record (six years, with 2025 incomplete) lacks the statistical power to establish a temporal trend.

Tidal flooding showed a bimodal seasonal pattern, with the highest number of flood-affected days occurring in June (43 days, 25.1%) and December–January (38 and 28 days, respectively). These seasonal peaks coincide with periods of elevated astronomical (spring) tides, with the December–January peak further coinciding with the northwest monsoon, which raises coastal water levels along Jakarta Bay. Of the 171 flood-affected days, 163 days or 95.3% were attributed exclusively to tidal inundation without rainfall contribution. The recorded inundation depths ranged from 10 to 80 cm. Pluit recorded a mean depth of 25.6 cm, while Penjaringan recorded a higher mean depth of 33.8 cm despite having fewer flood-affected days (Table 6).

Table 6. Recorded inundation depth statistics by Urban village, 2020–2025

Urban village	Mean Depth (cm)	Max Depth (cm)	Peak Event
Pluit	25.6	80	16–17 Dec 2024, RW 22
Penjaringan	33.8	50	Multiple events 2020–2024
Pejagalan	27.5	60	2020–2021 only
Kapuk Muara	15.0	25	2020–2021 only
Kamal Muara	15.0	15	Single event, 2021

The Hazard Index (HI) was calculated by normalizing three sub-indicators using min-max transformation and averaging them equally (Table 7). Pluit recorded the highest HI score of 1.000, which was classified as Very High. Penjaringan ranked second with an HI score of 0.400 and was classified as Moderate, driven primarily by its temporal consistency (norm = 0.600, with flood events recorded in four out of six observation years) and inundation depth (norm = 0.538), rather than its flood-day count (norm = 0.061). .

Table 7. Hazard index (HI)

Urban village	Total Days	N Years Affected	Max Depth (cm)	norm Total Days	norm N Years	norm Depth	HI	Class
Kamal Muara	1	1	15	0.000	0.000	0.000	0.000	Very Low
Kapuk Muara	6	2	25	0.034	0.200	0.154	0.129	Very Low
Pejagalan	5	2	60	0.027	0.200	0.692	0.306	Low
Penjaringan	10	4	50	0.061	0.600	0.538	0.400	Moderate
Pluit	149	6	80	1.000	1.000	1.000	1.000	Very High

3.1.2 Building the asset exposure profile and exposure index

The building inventory comprises 65,496 building polygons across four active land-use classifications, covering a total built-asset footprint of 1,187.70 ha (Table 8). Pluit recorded the largest total footprint at 282.40 ha, with the largest share coming from Residential land use (196.44 ha), followed by Commercial and Services (63.17 ha). Penjaringan and Kamal Muara recorded substantial Industrial and Infrastructure footprints, at 115.09 ha and 117.95 ha, respectively. The building density was highest in Pejagalan, reaching 11,138 units/km^2. This indicates that exposure is influenced not only by building extent but also by land-use composition and asset value, as a larger footprint does not necessarily translate into the highest exposed value.

Table 8. Building footprint area, unit count, and building density according to the urban village and land-use classification

Urban village	Industrial & Infrastructure (ha)	Commercial & Services (ha)	Government & Public Facilities (ha)	Residential (ha)	Total Built-Asset Footprint (ha)	Building Density (units/km^2)
Kamal Muara	117.95	31.16	6.31	75.96	231.38	418
Kapuk Muara	66.19	17.19	5.91	152.96	242.25	2,633
Pejagalan	21.62	46.06	6.49	107.31	181.48	11,138
Penjaringan	115.09	52.25	17.26	65.59	250.19	7,192
Pluit	13.45	63.17	9.34	196.44	282.40	2,182

The total replacement asset value for Penjaringan District was estimated at IDR 159.42 trillion (Table 9). At the urban village level, Penjaringan recorded the highest total asset value at IDR 36.43 trillion, followed by Pluit at IDR 34.82 trillion, Kamal Muara at IDR 34.23 trillion, Kapuk Muara at IDR 31.01 trillion, and Pejagalan at IDR 22.93 trillion. The weighted average unit costs underlying these values were spatially differentiated: Pluit exhibited the highest (IDR 11.015 million/m^2, with 87.5% of residential buildings classified as Type A+B), while Penjaringan exhibited the lowest (IDR 9.724 million/m^2, with 44.0% classified as Type D+E).

Table 9. Total replacement asset value by urban village and land-use classification (IDR Trillion)

Urban village	Industrial & Infrastructure (IDR T)	Commercial & Services (IDR T)	Government & Public Facilities (IDR T)	Residential (IDR T)	Total Asset Value (IDR T)
Kamal Muara	20.464	4.817	0.732	8.211	34.225
Kapuk Muara	11.484	2.658	0.686	16.187	31.014
Pejagalan	3.751	7.121	0.753	11.305	22.930
Penjaringan	19.968	8.078	2.002	6.378	36.426
Pluit	2.334	9.766	1.083	21.638	34.821
Total District	57.999	32.440	5.256	63.719	159.416

The Exposure Index (EI) was calculated using two normalized sub-indicators: total asset value and building density (Table 10). Penjaringan recorded the highest EI score at 0.816 and was classified as Very High. The remaining four urban villages were classified as Moderate, with EI scores ranging from 0.403 to 0.523. Pluit recorded an EI score of 0.523 despite having the largest built-asset footprint, while Pejagalan recorded an EI score of 0.500 due to its high building density.

Table 10. Exposure index (EI)

Urban village	Total Asset Value (IDR T)	Building Density (units/km^2)	norm Asset Value	norm Building Density	EI	Class
Kamal Muara	34.225	418	0.837	0.000	0.418	Moderate
Kapuk Muara	31.014	2,633	0.599	0.207	0.403	Moderate
Pejagalan	22.930	11,138	0.000	1.000	0.500	Moderate
Penjaringan	36.426	7,192	1.000	0.632	0.816	Very High
Pluit	34.821	2,182	0.881	0.165	0.523	Moderate

3.1.3 Social vulnerability profile and social vulnerability index

Raw social vulnerability indicator values are presented in Table 11. Penjaringan and Pejagalan recorded the highest population densities at 29,131.65 and 28,127.24 persons/km^2, respectively. Penjaringan recorded the highest slum settlement proportion at 90.49%, while Kapuk Muara recorded the highest malnutrition rate at 0.650 cases per 1,000 population.

Table 11. Raw social vulnerability indicator values by urban village

Urban village	Population Density (persons/km^2)	Slum Settlement Proportion (% of area)	Malnutrition Rate (cases/1,000 pop.)
Kamal Muara	1,760.59	15.75%	0.270
Kapuk Muara	4,745.67	2.48%	0.650
Pejagalan	28,127.24	9.76%	0.022
Penjaringan	29,131.65	90.49%	0.000
Pluit	7,756.29	0.00%	0.000
Min	1,760.59	0.00%	0.000
Max	29,131.65	90.49%	0.650

Following min-max normalization and equal-weight averaging, Penjaringan attained the highest Social Vulnerability Index (SVI) score of 0.667 and was classified as High (Table 12). Kapuk Muara and Pejagalan recorded Low SVI scores, at 0.379 and 0.368, respectively. Kamal Muara recorded a Very Low SVI score of 0.196, while Pluit had the lowest SVI score at 0.073 and was also classified as Very Low. Penjaringan's High SVI was primarily driven by the combination of the highest population density and the largest slum settlement proportion among the five urban villages (both normalized to 1.000), while its malnutrition indicator contributed the least (norm = 0.000).

Table 12. Social vulnerability index (SVI)

Urban village	norm Pop. Density	norm Slum Prop.	norm Malnutrition	SVI (mean)	Class	Dominant Driver
Kamal Muara	0.000	0.174	0.415	0.196	Very Low	Malnutrition rate
Kapuk Muara	0.109	0.027	1.000	0.379	Low	Malnutrition rate
Pejagalan	0.963	0.108	0.034	0.368	Low	Population density

 https://doi.org/10.61511/calamity.v4i1.2026.3759

Penjaringan	1.000	1.000	0.000	0.667	High	Pop. density + Slum proportion
Pluit	0.219	0.000	0.000	0.073	Very Low	Population density (only)

3.1.4 Risk index

The integrated Risk Index (RI), calculated as the unweighted arithmetic mean of the Hazard Index (HI), Exposure Index (EI), and Social Vulnerability Index (SVI), is presented in Table 13 and visualized spatially in Figure 2. Penjaringan recorded the highest composite RI score at 0.628 and was classified as High. Pluit ranked second with an RI score of 0.532 and was classified as Moderate. The remaining three urban villages recorded Low RI scores, namely Pejagalan at 0.391, Kapuk Muara at 0.304, and Kamal Muara at 0.205.

Penjaringan's composite RI was associated with a Moderate HI score of 0.400, a Very High EI score of 0.816, and a High SVI score of 0.667. In contrast, Pluit recorded the highest HI score at 1.000, but its EI and SVI scores were lower, at 0.523 and 0.073, respectively. This result shows that the urban village with the highest hazard score did not have the highest composite risk. The highest RI was found in Penjaringan, where high exposure and high social vulnerability occurred simultaneously. This reordering occurs because a hazard-only assessment would rank Pluit first, whereas the composite index registers Penjaringan's combination of Very High exposure and High social vulnerability, which jointly outweigh its Moderate hazard. This distinction is consequential for adaptation planning, as prioritizing interventions by hazard intensity alone would direct resources away from the urban village where flood impacts on people and assets are likely to be greatest.

Table 13. Composite risk index (RI)

Urban village	HI	HI Class	EI	EI Class	SVI	SVI Class	RI	RI Class	Rank
Kamal Muara	0.000	Very Low	0.418	Moderate	0.196	Very Low	0.205	Low	5
Kapuk Muara	0.129	Very Low	0.403	Moderate	0.379	Low	0.304	Low	4
Pejagalan	0.306	Low	0.500	Moderate	0.368	Low	0.391	Low	3
Penjaringan	0.400	Moderate	0.816	Very High	0.667	High	0.628	High	1
Pluit	1.000	Very High	0.523	Moderate	0.073	Very Low	0.532	Moderate	2

Note: The cell color in the RI Class column indicates the composite risk class — High (red), Moderate (orange), Low (green), and Very Low (dark green), where applicable

Figure 3 shows that the spatial distribution of composite risk differs from that of hazard alone. The HI map shows a strong concentration of tidal flood hazard in Pluit, which appears as the only urban village in the Very High hazard class. Penjaringan occupies a lower hazard class, while Kamal Muara, Kapuk Muara, and Pejagalan have lower hazard scores. This spatial pattern is consistent with the flood-affected day distribution presented in Table 5, where Pluit accounted for most recorded tidal flood events during the observation period.

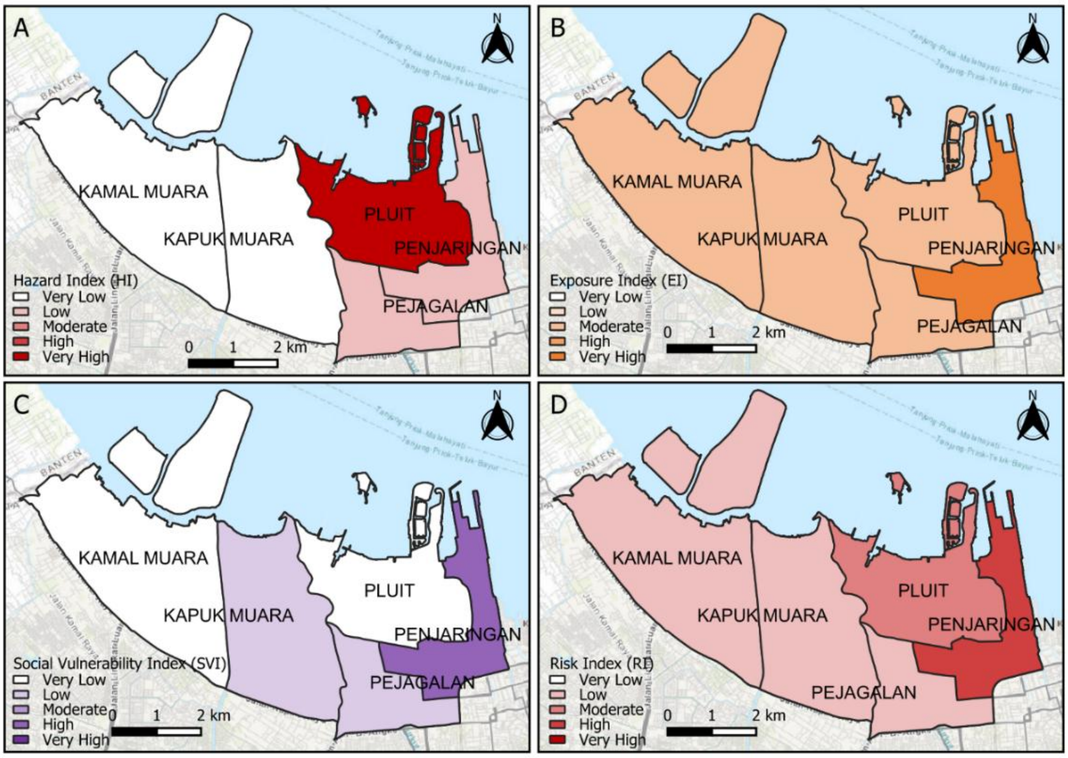

Spatial distribution of (A) Hazard Index, (B) Exposure Index, (C) Social Vulnerability Index, and (D) Risk Index across five kelurahan of Penjaringan District. Color ramps: red (HI, RI), orange (EI), purple (SVI); darker shading indicates higher index values.

Fig. 3. Spatial distribution of flood risk indices

The EI map shows a different spatial pattern. Penjaringan appears as the urban village with the highest exposure level, corresponding to its Very High EI score. Meanwhile, Pluit, Kamal Muara, Kapuk Muara, and Pejagalan are classified as Moderate exposure. The SVI map further differentiates the risk profile of the district, with Penjaringan appearing as the most socially vulnerable urban village, while Pluit records the lowest vulnerability level. The RI map shows Penjaringan as the highest-risk urban village, followed by Pluit. This spatial pattern suggests that adaptation priorities should focus on areas where multiple risk dimensions converge, as in Penjaringan, rather than on hazard hotspots alone, as a hazard-based reading would single out Pluit.

Table 14. Sensitivity analysis of composite risk index

Urban village	S0 Equal		S1 Hazard-dom.		S2 Exposure-dom.		S3 Vuln.-dom.		Max Shift
	RI	Rank	RI	Rank	RI	Rank	RI	Rank	
Kamal Muara	0.205	5	0.153	5	0.258	5	0.203	5	0
Kapuk Muara	0.304	4	0.260	4	0.329	4	0.323	4	0
Pejagalan	0.391	3	0.370	3	0.418	3	0.386	3	0
Penjaringan	0.628	1	0.571	2	0.675	1	0.637	1	1
Pluit	0.532	2	0.649	1	0.530	2	0.417	2	1

Note: RI Class color follows the classification thresholds in Table 13. S0 = equal weights (HI = EI = SVI = 1/3); S1 = hazard-dominant (HI = 0.50, EI = SVI = 0.25); S2 = exposure-dominant (EI = 0.50, HI = SVI = 0.25); S3 = vulnerability-dominant (SVI = 0.50, HI = EI = 0.25). Max Shift = maximum rank change across all four scenarios.

Table 14 presents the sensitivity analysis results. Kamal Muara, Kapuk Muara, and Pejagalan maintained the same ranking across all weighting scenarios, indicating that their relative positions were stable under alternative weighting assumptions. Under the hazard-dominant scenario, the only rank change occurred between Penjaringan and Pluit, where

Pluit became Rank 1 with an RI score of 0.649, while Penjaringan became Rank 2 with an RI score of 0.571. Under the equal-weight, exposure-dominant, and vulnerability-dominant scenarios, Penjaringan remained the highest-ranked urban village. Penjaringan retains the top rank under these scenarios because it holds the highest EI and SVI simultaneously, so any weighting scheme not dominated by the hazard component preserves its position; only the hazard-dominant scenario, which halves the combined influence of these two dimensions, allows Pluit's maximum HI to prevail. The maximum rank shift across all four scenarios was one position. This indicates that the composite RI ranking was relatively stable, although the top position was sensitive to the hazard component's weighting. . Therefore, the equal-weight scenario was retained as the reference scenario for the subsequent typology and quadrant analyses.

Table 15. Risk typology classification by urban village in Penjaringan District

Urban village	RI (Class)	Dominant Driver	Typology
Kamal Muara	Low	EI	Exposure-Dominant
Kapuk Muara	Low	EI	Exposure-Dominant
Pejagalan	Low	EI	Exposure-Dominant
Penjaringan	High	EI + SVI	Compound Risk
Pluit	Moderate	HI	Hazard-Dominant

Note: Compound Risk refers to an urban village where two or more component indices reach the High or Very High class. RI Class color follows the classification thresholds in Table 13.

The risk typology classification is presented in Table 15. Penjaringan was classified as a Compound Risk because its EI and SVI simultaneously reached the High or Very High class. This indicates that Penjaringan's risk profile was driven by the combined contribution of high asset exposure and high social vulnerability rather than a single component. For flood risk management, this classification implies that single-sector interventions would be insufficient for Penjaringan; risk reduction requires pairing physical flood protection with measures that reduce exposure and strengthen the adaptive capacity of its vulnerable population. Pluit was classified as Hazard-Dominant because HI was its highest component index, reflecting the concentration of recorded tidal flood events in this urban village. Kamal Muara, Kapuk Muara, and Pejagalan were classified as Exposure-Dominant because EI was the highest component index in each urban village.

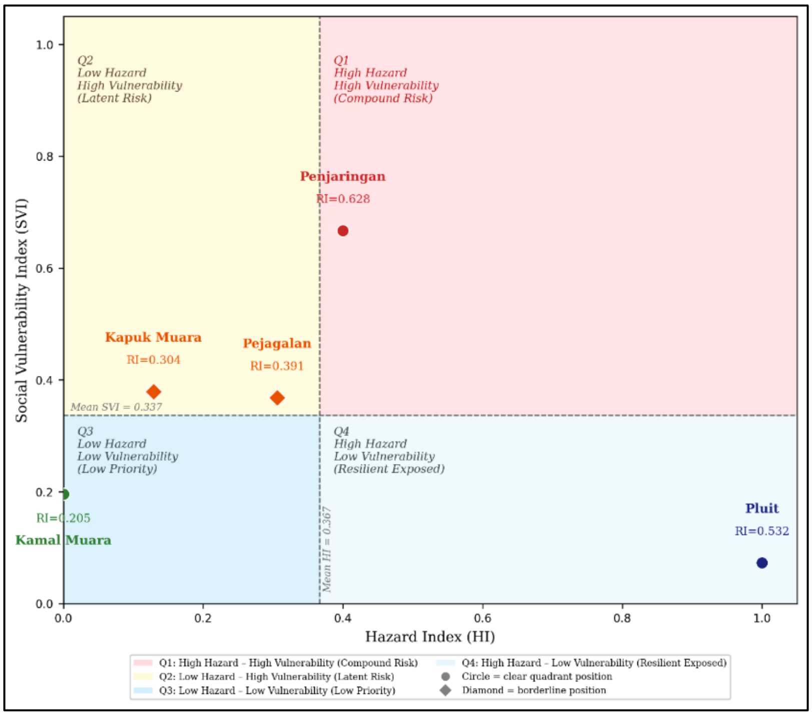

Fig. 4. Hazard-Vulnerability quadrant analysis

Although these three urban villages shared the same Exposure-Dominant typology, their RI classes remained Low, indicating that high exposure alone did not translate into high composite risk when hazard and social vulnerability scores were comparatively lower. Pejagalan showed the highest RI among the Exposure-Dominant urban villages, while Kamal Muara recorded the lowest RI. Overall, the typology classification shows that the dominant risk driver varies across urban villages, with Penjaringan characterized by compound exposure-vulnerability risk, Pluit by hazard concentration, and the remaining urban villages by exposure-led risk profiles. These different risk profiles indicate that adaptation strategies should be differentiated accordingly, with hazard reduction prioritized in Pluit, combined exposure and vulnerability reduction emphasized in Penjaringan, and asset-protection measures suited to the exposure-led profiles of the remaining urban villages.

Figure 4 and Table 16 present the hazard-vulnerability quadrant analysis. The quadrant boundaries were determined using the district mean values of HI and SVI (mean HI = 0.367; mean SVI = 0.337), which serve as thresholds distinguishing urban villages with above-average and below-average hazard and vulnerability conditions. Penjaringan was located in Quadrant 1 (High Hazard–High Vulnerability), as both its HI (0.400) and SVI (0.667) exceed the district mean. Pluit was located in Quadrant 4 (High Hazard–Low Vulnerability), recording the maximum HI with SVI well below the mean. Kamal Muara was located in Quadrant 3 (Low Hazard–Low Vulnerability), with both indices below the district mean. Kapuk Muara was classified as borderline Quadrant 2 (Low Hazard–High Vulnerability), because its SVI (0.379) is only marginally above the mean (0.337). Pejagalan was classified in Quadrant 2 (Low Hazard–High Vulnerability), with HI below the mean (0.306 < 0.367) and SVI above the mean (0.368 > 0.337).

Table 16. Hazard–vulnerability quadrant positions per urban village in the Penjaringan District

Urban village	HI (x)	SVI (y)	Quadrant	Quadrant Label	Notes
Kamal Muara	0.000	0.196	Q3	Low Hazard – Low Vulnerability	Clear Q3; HI and SVI both below the district mean
Kapuk Muara	0.129	0.379	Q2	Low Hazard – High Vulnerability	Borderline Q2; SVI = 0.379, marginally above the mean (0.337)
Pejagalan	0.306	0.368	Q2	Low Hazard – High Vulnerability	HI below mean (0.367); SVI above mean (0.337)
Penjaringan	0.400	0.667	Q1	High Hazard – High Vulnerability	Clear Q1; both HI and SVI above the district mean
Pluit	1.000	0.073	Q4	High Hazard – Low Vulnerability	Clear Q4; maximum HI, SVI well below the mean

Quadrant boundaries: Mean HI = 0.367; Mean SVI = 0.337.

3.2 Discussion

Consistent with the objective of developing an integrated flood risk assessment framework, the results demonstrate that coastal flood risk in Penjaringan District is shaped by the interaction of hazard, exposure, and vulnerability rather than by hazard frequency alone.Although Pluit recorded the highest Hazard Index (HI = 1.000) and accounted for the largest proportion of flood-affected days, the highest composite Risk Index was observed in Penjaringan (RI = 0.628). This confirms that disaster risk is produced through the interaction between hazard, exposure, and vulnerability, rather than by physical hazard alone (Bin et al., 2023). This study directly addresses the methodological gap identified in previous Indonesian coastal flood studies by empirically combining historical tidal flood records, asset exposure valuation, and social vulnerability indicators into a composite urban village-level risk index by combining historical tidal flood records, asset exposure valuation, and social vulnerability indicators into a composite urban village-level risk index (Ariyani et al., 2024; Hastuti et al., 2022; Mutia Gunandar et al., 2024; Putiamini et al., 2023). Therefore, the integration of HI, EI, and SVI provides a more comprehensive basis for understanding coastal flood risk than a single-dimensional hazard assessment. This integrated framework allows decision-makers to identify priority areas where hazardous conditions coincide with high asset exposure and limited community coping capacity, which a hazard-only assessment would overlook.

Pluit represents a hazard-dominant risk profile. The urban village recorded the most frequent tidal flood events and was the only area classified as Very High in the Hazard Index. This indicates that recurrent tidal inundation remains a major physical threat in Pluit. In contrast, Penjaringan achieved the highest composite risk because its moderate hazard conditions were amplified by very high asset exposure and high social vulnerability. Repeated tidal flooding can cause cumulative disruption to mobility (Yao et al., 2024), housing (McAlpine & Porter, 2018; Utami et al., 2021), infrastructure (Rezvani et al., 2024), andlocal economic activity (Dong et al., 2024), even when individual flood events are not extreme. However, Pluit also recorded the lowest Social Vulnerability Index (SVI = 0.073), which reduced its composite RI to the Moderate class. This suggests that high physical exposure to flooding does not automatically produce the highest composite risk when social vulnerability is relatively low (Fox et al., 2024) Consistent with its Hazard-Dominant classification, Pluit's risk is mainly related to the management of recurrent tidal hazard through flood protection infrastructure, drainage systems, pumping capacity, and tidal monitoring

In contrast, Penjaringan represents the district's most critical compound risk profile. Although its HI score was lower than that of Pluit's, Penjaringan had the highest Exposure Index (EI = 0.816) and the highest Social Vulnerability Index (SVI = 0.667). This combination indicates that Penjaringan's risk is not driven by flood frequency alone, but by the simultaneous concentration of economic assets and socially vulnerable populations. Social vulnerability studies argue that communities with limited resources, poor settlement quality, and high demographic pressure tend to experience greater losses and slower recovery after flood events (Fox et al., 2024). In Penjaringan, high population density and extensive slum settlement area indicate limited household-level coping capacity and greater potential disruption if tidal inundation expands or intensifies. Thus, Penjaringan should be interpreted as a latent high-risk area, where future changes in flood extent may produce severe social and economic consequences.

One of the central findings of this study is the contrast between Pluit and Penjaringan. A hazard-only approach would identify Pluit as the main priority because it records the most frequent tidal flooding. However, the composite RI shows that Penjaringan has a higher overall risk because high exposure and high vulnerability occur simultaneously. This finding is consistent with the risk governance literature, which argues that adaptation priorities should consider not only where hazards occur but also where exposed assets and vulnerable communities are concentrated (Fox et al., 2024). In practical terms, an area with less frequent flooding may still require urgent attention for adaptation if its potential losses and social constraints are greater. Therefore, the results support the use of multi-dimensional risk assessment for spatially targeted and socially equitable coastal adaptation planning (Anderson et al., 2024).

The results of exposure and vulnerability further explain why Penjaringan ranks highest in composite risk. Pluit recorded the largest built-asset footprint, but Penjaringan recorded the highest total asset value and EI, indicating that exposure is shaped not only by built-up area but also by land-use composition and asset value (Bonatz et al., 2024). Simultaneously, Penjaringan's high SVI is associated with very high population density and extensive slum settlement area, showing that social vulnerability is spatially uneven across the district. The residential building-type distribution corroborates this pattern independently, as Penjaringan's predominance of smaller Type D–E dwellings is consistent with its high social vulnerability profile. Kapuk Muara illustrates a different vulnerability pathway, where malnutrition prevalence contributes more strongly to its SVI profile. . These findings suggest that exposure and vulnerability should be interpreted as multidimensional conditions, rather than as single-indicator measures (Mah et al., 2023). Therefore, the combination of high asset exposure and high social vulnerability makes Penjaringan more critical than areas where only one risk dimension is dominant.

The sensitivity analysis strengthens the robustness of the composite RI results. Kamal Muara, Kapuk Muara, and Pejagalan maintained the same ranking across all weighting scenarios, while the only rank change occurred between Penjaringan and Pluit under the hazard-dominant scenario. This indicates that the relative risk positions are generally stable, although the top priority becomes sensitive when hazard is assigned a dominant weight. Such sensitivity is common in composite index construction because weighting choices reflect normative and policy assumptions about which risk dimension should receive greater importance (Kelemen et al., 2024). Penjaringan remains the highest-ranked urban village under the equal-weight, exposure-dominant, and vulnerability-dominant scenarios suggests that its priority status is not merely an artifact of one weighting model.

The risk typology and hazard-vulnerability quadrant analyses provide a practical basis for developing differentiated adaptation strategies. Penjaringan was classified as a Compound Risk, indicating that adaptation should address both the physical and social dimensions of risk. Infrastructure-based flood control alone may be insufficient in compound-risk areas if it is not accompanied by settlement upgrading, vulnerability reduction, and community preparedness (Bhanye, 2025). Therefore, adaptation in Penjaringan should combine flood protection measures with actions that improve settlement conditions and reduce social vulnerability. Pluit, classified as Hazard-Dominant in Quadrant 4 (High Hazard–Low Vulnerability), requires adaptation focused primarily on managing recurrent tidal inundation through structural measures: strengthening sea walls, expanding pumping capacity, improving drainage systems, and establishing early warning and tidal monitoring. Kamal Muara, Kapuk Muara, and Pejagalan, all classified as Exposure-Dominant, face lower current risk but require proactive land-use management and asset protection to prevent future risk accumulation as relative sea levels continue to rise. Pejagalan and Kapuk Muara, both positioned in Quadrant 2 (Low Hazard–High Vulnerability), indicate that social vulnerability dimensions should be monitored alongside asset exposure. For Kapuk Muara specifically, the malnutrition-driven SVI profile suggests that health and nutrition service access should be incorporated into adaptation planning alongside physical measures.

The results of this study should be interpreted as an initial prioritization tool rather than a final set of adaptation interventions, identifying where more detailed technical, socioeconomic, and institutional assessments are needed. If planning attention is based only on observed flood frequency, areas with lower current hazard but higher exposure and social vulnerability, as illustrated by Penjaringan, risk being systematically underrepresented in coastal risk assessment. This constitutes an equity inversion that multi-dimensional frameworks are specifically designed to prevent(Anderson et al., 2024).

This study contributes a data-limited and replicable approach for prioritizing urban coastal flood risk. The framework provides a practical alternative for local governments that do not yet have access to detailed hydrodynamic simulation by integrating official flood records, spatial building data, asset valuation, and urban-village-level social indicators. Thus, the main contribution of this study lies not only in identifying which urban village has the highest risk but also in demonstrating how a data-limited integrated framework can reveal spatial mismatches between hazard concentration, economic exposure, and social vulnerability in coastal urban areas.

However, the results should be interpreted within several limitations. The flood record covers only January 2020 to September 2025, thus limiting the statistical power of long-term trend detection. Because hydrodynamic modeling was not included, exposure values represent potential asset exposure rather than event-specific damage estimates. In addition, the SVI is limited to three indicators due to data availability. Furthermore, analysis at the urban village level may mask within-village spatial heterogeneity, a limitation inherent to the available administrative data resolution. Future research should extend the flood observation period, integrate hydrodynamic simulation, include broader socioeconomic indicators, and consider stakeholder-based weighting methods to improve the available administrative data resolution.

4. Conclusions

This study applied an integrated coastal flood risk assessment framework to Penjaringan District, North Jakarta, by combining the Hazard Index (HI), Exposure Index (EI), and Social Vulnerability Index (SVI) into a composite Risk Index (RI) at the urban village level. Using routinely produced administrative and spatial data, the study shows that coastal flood risk in Penjaringan District cannot be explained by tidal flood frequency alone. The main finding is a spatial mismatch between the urban village with the highest hazard and the urban village with the highest composite risk. Pluit recorded the highest hazard level, accounting for 87.1% of all flood-affected days and reaching a maximum HI score of 1.000. However, Penjaringan recorded the highest composite RI score of 0.628, driven by Very High exposure (EI = 0.816) and High social vulnerability (SVI = 0.667). This highlights that flood risk should be assessed beyond hazard frequency alone. These findings confirm the importance of integrating hazard, exposure, and vulnerability in coastal flood risk assessment. A hazard-only approach would identify Pluit as the primary risk area, while the composite RI reveals Penjaringan as the most critical risk area because of the co-occurrence of high asset exposure, extreme population density, and extensive slum settlement area. This result addresses the methodological gap in previous Indonesian coastal flood studies, which have often separately examined tidal inundation, exposure, or vulnerability. This integrated approach provides a more complete understanding of coastal flood risk.

Differentiated adaptation priorities are recommended for each urban village based on the composite risk profiles. As the highest-risk area with a Compound Risk profile, Penjaringan requires simultaneous intervention across physical and social dimensions: slum settlement upgrading, community flood preparedness, and protection of high-value industrial and commercial assets. As a hazard-dominant area, Pluit should prioritize structural flood protection, pumping capacity, drainage improvement, and tidal early warning systems. Kamal Muara, Kapuk Muara, and Pejagalan, classified as Exposure-Dominant with Low composite risk, require proactive land-use management and asset monitoring to prevent future risk accumulation as relative sea levels continue to rise.

This study also demonstrates that a data-limited approach can provide meaningful risk prioritization when detailed hydrodynamic modeling is unavailable. This makes the framework useful as an initial risk assessment and preliminary adaptation prioritization tool in coastal urban contexts with limited data. To replicate this framework in other Indonesian coastal districts, the minimum data requirements are as follows: (1) a multi-year administrative flood event record with inundation depth at the urban village level; (2) a georeferenced building polygon layer with land-use classification; (3) official building replacement unit costs; and (4) urban village level social indicators covering at least population density, settlement quality, and a health proxy. Institutionally, access to these datasets requires formal coordination with the BPBD, DCKTRP, or equivalent spatial planning agency, and the BPS at the city level, all of which are routinely produced by Indonesian local governments and accessible via formal academic research requests.

Nevertheless, the findings should be interpreted cautiously. The flood record covers only January 2020 to September 2025, with the 2025 record incomplete. Exposure values represent potential asset exposure rather than event-specific losses, and due to data availability, the SVI is limited to three indicators. Future research should extend the flood record, integrate hydrodynamic modeling, include broader socioeconomic vulnerability indicators, and apply stakeholder-based weighting methods. These improvements can increase the accuracy of future risk assessments. These findings suggest that adaptation prioritization in Penjaringan District should extend beyond hazard-focused flood control to include settlement upgrading and social vulnerability reduction, while hazard-dominant areas such as Pluit require continued investment in structural flood management. This distinction offers a practical basis for spatially differentiated adaptation planning in similarly data-limited coastal contexts.

Acknowledgement

The authors would like to thank the Provincial Government of DKI Jakarta for providing access to official data used in this study. The authors also acknowledge the support of the Graduate School of Environmental Science, Universitas Indonesia.

Author Contribution

Conceptualization, Aswin Kurnia Ramadhan; Methodology, Aswin Kurnia Ramadhan; Software, Aswin Kurnia Ramadhan; Formal Analysis, Aswin Kurnia Ramadhan; Investigation, Aswin Kurnia Ramadhan; Data Curation, Aswin Kurnia Ramadhan; Writing – Original Draft Preparation, Aswin Kurnia Ramadhan; Writing – Review & Editing, Wezia Berkademi and Rachmadhi Purwana; Visualization, Aswin Kurnia Ramadhan; Supervision, Wezia Berkademi and Rachmadhi Purwana; Project Administration, Aswin Kurnia Ramadhan.

Funding

This research received no external funding.

Ethical Review Board Statement

Not available. This study used only secondary spatial and administrative data obtained from official government sources. No primary data collection involving human subjects was conducted**.**

Informed Consent Statement

Not available.

Data Availability Statement

The tidal flood records used in this study were obtained from the Regional Disaster Management Agency of DKI Jakarta Province (BPBD DKI Jakarta) via formal request for academic research purposes and are not publicly available. Building polygon data and the slum settlement map were provided by the Department of Spatial Planning and Land (DCKTRP) DKI Jakarta. Social vulnerability indicators were sourced from BPS Kota Jakarta Utara, *Kecamatan Penjaringan Dalam Angka* 2024, available at bps.go.id. Building replacement unit costs were derived from the Governor of DKI Jakarta Decree No. 580/2025 (SHSBGN). Building footprint data supplementation used OpenStreetMap (openstreetmap.org). Flood depth-damage parameters were sourced from Huizinga et al. (2017), available at the Joint Research Centre (JRC) Data Catalogue.

Conflicts of Interest

The authors declare no conflict of interest.

Declaration of Generative AI Use

During the preparation of this work, the authors used Grammarly to assist in improving grammar, clarity, and academic tone of the manuscript. After using this tool, the authors reviewed and edited the content as needed and took full responsibility for the content of the publication."

Open Access

References

Acosta-Morel, M., McNulty, V. P., Lummen, N., Schill, S. R., & Beck, M. W. (2021). Shoreline Solutions: Guiding Efficient Data Selection for Coastal Risk Modeling and the Design of Adaptation Interventions. *Water*, *13*(6), 875. https://doi.org/10.3390/w13060875

An, Y., Tan, X., Gu, B., & Zhu, K. (2020). Flood risk assessment using the CV-TOPSIS method for the Belt and Road Initiative: an empirical study of Southeast Asia. *Ecosystem Health and Sustainability*, *6*. https://doi.org/10.1080/20964129.2020.1765703

Anderson, M., Conrow, L., Hobbs, M., Paulik, R., Blackett, P., & Logan, T. (2024). Distributional justice and climate risk assessment: An analysis of disparities within direct and indirect risk. *Risk Analysis*, *45*, 3354–3374. https://doi.org/10.1111/risa.17664

Anindita, R. M., Susilowati, I., & Muhammad, F. (2020). Flood risk spatial index analysis in the coastal Pekalongan, Central Java, Indonesia. *E3S Web of Conferences*. https://doi.org/10.1051/e3sconf/202020206028

Ariyani, D., Purwanto, Muh. Y. J., Sunarti, E., Perdinan, P., & Juniati, A. (2024). Integrated flood hazard assessment using multi-criteria analysis and geospatial modeling. *Journal of Degraded and Mining Lands Management*. https://doi.org/10.15243/jdmlm.2024.114.6121

Asmadin, Siregar, V. P., Sofian, I., Jaya, I., & Wijanarto, A. B. (2021). The Change in Elevation, Land Subsidence and Local Sea Level Rise Using Coastal Response Model in Jakarta. *IOP Conference Series: Earth and Environmental Science*, *750*(1). https://doi.org/10.1088/1755-1315/750/1/012010

Begum, A., Lempert, R., Ali, E., Benjaminsen, T. A., Bernauer, T., Cramer, W., Cui, X., Mach, K., Nagy, G., Stenseth, N. C., Sukumar, R., & Wester, P. (2023). Point of Departure and Key Concepts. In H.-O. Pörtner, D. C. Roberts, M. Tignor, E. S. Poloczanska, K. Mintenbeck, A. Alegría, M. Craig, S. Langsdorf, S. Löschke, V. Möller, A. Okem, & B. Rama (Eds.), *Climate Change 2022 – Impacts, Adaptation and Vulnerability* (pp. 121–196). Cambridge University Press. https://doi.org/10.1017/9781009325844.003

Bhanye, J. (2025). A review study on community-based flood adaptation in informal settlements in the Global South. *Discover Sustainability*, *6*. https://doi.org/10.1007/s43621-025-01449-6

Bin, L., Xu, K., Pan, H., Zhuang, Y., & Shen, R. (2023). Urban flood risk assessment characterizing the relationship among hazard, exposure, and vulnerability. *Environmental Science and Pollution Research*, *30*(36), 86463–86477. https://doi.org/10.1007/s11356-023-28578-7

BNPB. (2025). *Indeks Risiko Bencana Indonesia 2024*. Badan Nasional Penanggulangan Bencana. https://inarisk.bnpb.go.id/IRBI-2024/mobile/index.html

Bonatz, H., Reimann, L., & Vafeidis, A. T. (2024). Comparing built-up area datasets to assess urban exposure to coastal hazards in Europe. *Scientific Data*, *11*(1), 499. https://doi.org/10.1038/s41597-024-03339-4

Bott, L.-M., Schöne, T., Illigner, J., Haghshenas Haghighi, M., Gisevius, K., & Braun, B. (2021). Land subsidence in Jakarta and Semarang Bay – The relationship between physical processes, risk perception, and household adaptation. *Ocean & Coastal Management*, *211*, 105775. https://doi.org/10.1016/j.ocecoaman.2021.105775

Causevic, A., LoCastro, M., David, D., Selvakkumaran, S., & Gren, Å. (2021). Financing resilience efforts to confront future urban and sea-level rise flooding: Are coastal megacities in Association of Southeast Asian Nations doing enough? *Environment and Planning B: Urban Analytics and City Science*, *48*(5), 989–1010. https://doi.org/10.1177/2399808321994437

Dong, W. S., Ismailluddin, A., Yun, L. S., Ariffin, E. H., Saengsupavanich, C., Maulud, K. A., Ramli, M. Z., Miskon, M., Jeofry, M., Mohamed, J., Mohd, F., Hamzah, T. S. B., & Yunus, K. (2024). The impact of climate change on coastal erosion in Southeast Asia and the compelling need to establish robust adaptation strategies. *Heliyon*, *10*. https://doi.org/10.1016/j.heliyon.2024.e25609

Eaves, A., Kench, P. S., McDonald, G., Dickson, M. E., & Storey, B. (2023). Modelling Economic Risk to Sea-level Rise and Storms at the Coastal Margin. *Journal of Flood Risk Management*, *18*(1). https://doi.org/10.1111/jfr3.12903

FathiAzar, A. (2025). A Micro-Scale Framework for Evaluating the Cost-Effectiveness of Building-Level Floodproofing Measures. *Journal of Flood Risk Management*, *18*(3). https://doi.org/10.1111/jfr3.70126

Flanagan, B. E., Gregory, E. W., Hallisey, E. J., Heitgerd, J. L., & Lewis, B. (2011). A Social Vulnerability Index for Disaster Management. *Journal of Homeland Security and Emergency Management*, *8*(1). https://doi.org/10.2202/1547-7355.1792

Fox, S., Agyemang, F., Hawker, L., & Neal, J. (2024). Integrating social vulnerability into high-resolution global flood risk mapping. *Nature Communications* , *15*(1). https://doi.org/10.1038/s41467-024-47394-2

Harintaka, H., Suhadha, A. G., Syetiawan, A., Ardha, M., & Rarasati, A. (2024). Current land subsidence in Jakarta: a multi-track SBAS InSAR analysis during 2017–2022 using C-band SAR data. *Geocarto International*, *39*(1). https://doi.org/10.1080/10106049.2024.2364726

Hasibuan, H. S., Elizandri, B. N., Asrofani, F. W., & Putra, G. A. Y. (2025). Potential application of rain water harvesting technology as an alternative clean water source to mitigate land subsidence. *Global Journal of Environmental Science and Management*, *11*(1), 277–294. https://doi.org/10.22034/gjesm.2025.01.17

Hasibuan, H. S., Tambunan, R. P., Rukmana, D., Permana, C. T., Elizandri, B. N., Putra, G. A. Y., Wahidah, A. N., & Ristya, Y. (2023). Policymaking and the spatial characteristics of land subsidence in North Jakarta. *City and Environment Interactions*, *18*. https://doi.org/10.1016/j.cacint.2023.100103

Hastuti, A. W., Nagai, M., & Suniada, K. (2022). Coastal Vulnerability Assessment of Bali Province, Indonesia Using Remote Sensing and GIS Approaches. *Remote. Sens.*, *14*, 4409. https://doi.org/10.3390/rs14174409

Huizinga, J., de Moel, H., & Szewczyk, W. (2017). Global flood depth-damage functions: Methodology and the database with guidelines. In *EUR 28552 EN*. Publications Office of the European Union. https://doi.org/10.2760/16510

Hussain, Md. M., & Mahmud, I. (2019). pyMannKendall: A python package for non parametric Mann Kendall family of trend tests. *Journal of Open Source Software*, *4*(39), 1556. https://doi.org/10.21105/joss.01556

IPCC. (2023a). *Climate Change 2021 – The Physical Science Basis*. Intergovernmental Panel on Climate Chang. https://doi.org/10.1017/9781009157896

IPCC. (2023b). *Climate Change 2022 – Impacts, Adaptation and Vulnerability: Working Group II Contribution to the Sixth Assessment Report of the Intergovernmental Panel on Climate Change*. Intergovernmental Panel on Climate Change. https://doi.org/DOI: 10.1017/9781009325844

Jevrejeva, S., Jackson, L. P., Riva, R. E. M., Grinsted, A., & Moore, J. C. (2016). Coastal sea level rise with warming above 2 °C. *Proceedings of the National Academy of Sciences of the United States of America*, *113*(47), 13342–13347. https://doi.org/10.1073/pnas.1605312113

Johnson, D., Blackett, P., Allison, A. E. F., & Broadbent, A. M. (2023). Measuring Social Vulnerability to Climate Change at the Coast: Embracing Complexity and Context for More Accurate and Equitable Analysis. In *Water (Switzerland)* (Vol. 15, Number 19). Multidisciplinary Digital Publishing Institute (MDPI). https://doi.org/10.3390/w15193408

Kelemen, A., Szabo, Z., Bozóki, S., Szádoczki, Z., & Hartvig, Á. (2024). A sensitivity analysis of composite indicators: Min/max thresholds. *Environmental and Sustainability Indicators*. https://doi.org/10.1016/j.indic.2024.100453

Kim, J., & Gim, T. (2020). Assessment of social vulnerability to floods on Java, Indonesia. *Natural Hazards*, *102*, 101–114. https://doi.org/10.1007/s11069-020-03912-1

Mah, J., Penwarden, J., Pott, H., Theou, O., & Andrew, M. (2023). Social vulnerability indices: a scoping review. *BMC Public Health*, *23*. https://doi.org/10.1186/s12889-023-16097-6

McAlpine, S., & Porter, J. (2018). Estimating Recent Local Impacts of Sea-Level Rise on Current Real-Estate Losses: A Housing Market Case Study in Miami-Dade, Florida. *Population Research and Policy Review*, *37*, 871–895. https://doi.org/10.1007/s11113-018-9473-5

Mita, K. S., Orton, P., Montalto, F., Saleh, F., & Rockwell, J. (2023). Sea Level Rise-Induced Transition from Rare Fluvial Extremes to Chronic and Compound Floods. *Water (Switzerland)*, *15*(14). https://doi.org/10.3390/w15142671

Mutia Gunandar, C., Hasibuan, H. S., Tambunan, R. P., & Gunandar, C. M. (2024). Flood Vulnerability In Jakarta Coastal Settlement: A Study At Kalibaru Subdistrict, North Jakarta, Indonesia. In *Journal of the Malaysian Institute of Planners VOLUME* (Vol. 22). https://doi.org/10.21837/pm.v22i34.1584

Nashrrullah, S., Monika Pasaribu, J., Hazarika, M. K., & Samarakoon, L. (2013). STUDY ON FLOOD INUNDATION IN PEKALONGAN, CENTRAL JAVA. In *International Journal of Remote Sensing and Earth Sciences* (Vol. 10, Number 2). https://doi.org/10.30536/ijreses.v10i2.14074

Nurhidayah, L., Davies, P., Alam, S., Saintilan, N., & Triyanti, A. (2022). Responding to sea level rise: challenges and opportunities to govern coastal adaptation strategies in Indonesia. *Maritime Studies*, *21*(3), 339–352. https://doi.org/10.1007/s40152-022-00274-1

Paranunzio, R., Guerrini, M., Dwyer, E., Alexander, P. J., & O'Dwyer, B. (2022). Assessing Coastal Flood Risk in a Changing Climate for Dublin, Ireland. *Journal of Marine Science and Engineering*, *10*(11), 1715. https://doi.org/10.3390/jmse10111715

Pradana, A., Yew, Y., Demetriou, C., Prayitno, H., Delgado, R., González, P., & Utami, R. (2023). Risk Mapping of Coastal Cities that Sinking Faster than Sea-Level Rise by 2050: The Case of Jakarta and Semarang. *Prehospital and Disaster Medicine*, *38*. https://doi.org/10.1017/S1049023X23003278

Putiamini, S., Patria, M. P., Soesilo, T. E. B., & Karsidi, A. (2023). Coastal Vulnerability Assessment To Tidal (Rob) Flooding In Indramayu Coast, West Java, Indonesia. *Indonesian Journal of Geography*, *55*(3), 517–526. https://doi.org/10.22146/ijg.65549

Reisinger, A., Howden, M., Vera, C., & others. (2020). *The Concept of Risk in the IPCC Sixth Assessment Report: A Summary of Cross-Working Group Discussions*. https://www.ipcc.ch/site/assets/uploads/2021/02/Risk-guidance-FINAL_15Feb2021.pdf

Rezvani, S., Silva, M. J. F., & De Almeida, N. M. (2024). Urban Resilience Index for Critical Infrastructure: A Scenario-Based Approach to Disaster Risk Reduction in Road Networks. *Sustainability*. https://doi.org/10.3390/su16104143

Setiadi, R., Baumeister, J., Burton, P., & Nalau, J. (2020). Extending Urban Development on Water: Jakarta Case Study. *Environment and Urbanization ASIA*, *11*(2), 247–265. https://doi.org/10.1177/0975425320938539

Siegert, M., & Pearson, P. (2021). Reducing Uncertainty in 21st Century Sea-Level Predictions and Beyond. *Frontiers in Environmental Science*, *9*. https://doi.org/10.3389/fenvs.2021.751978

Solecki, W., & Friedman, E. (2021). At the Water's Edge: Coastal Settlement, Transformative Adaptation, and Well-Being in an Era of Dynamic Climate Risk. *Annual Review of Public Health*, *42*(1), 211–232. https://doi.org/10.1146/annurev-publhealth-090419-102302

Suroso, D. S. A., & Firman, T. (2018). The role of spatial planning in reducing exposure towards impacts of global sea level rise case study: Northern coast of Java, Indonesia. *Ocean and Coastal Management*, *153*, 84–97. https://doi.org/10.1016/j.ocecoaman.2017.12.007

Turner, G., Kovats, S., Brisley, R., Brown, S., Landeg, O., & O'Connor, L. (2025). Can We Adapt Fairly? Scoping Review of Health Equity Implications of Flood Risk in Coastal Communities. *BMJ Public Health*, *3*(2), e002588. https://doi.org/10.1136/bmjph-2025-002588

UNDRR. (2015). *Sendai Framework for Disaster Risk Reduction 2015–2030*. United Nations Office for Disaster Risk Reduction. https://www.undrr.org/publication/sendai-framework-disaster-risk-reduction-2015-2030

Utami, W., Wibowo, Y., & Permadi, F. (2021). The Impact of Tidal Flooding on Decreasing Land Values in the Areas of Tugu District, Semarang City. *Jurnal Ilmu Lingkungan*. https://doi.org/10.14710/jil.19.1.10-20

Warren-Myers, G., & Cradduck, L. (2023). Tackling the Wicked Challenge Of climate Change Risks to Property: Are Australian Valuers Prepared? *Journal of Property Investment & Finance*, *41*(4), 429–452. https://doi.org/10.1108/jpif-12-2022-0090

Yao, Q., Shan, X., Li, M., & Wang, J. (2024). The Impact of Floods on the Mobility of Automobile Commuters in Shanghai Under Climate Change. *International Journal of Disaster Risk Science*, *15*, 986–1000. https://doi.org/10.1007/s13753-024-00604-3

Yusuf, R. A., Pratama, M. B., Karjadi, E. A., & Takagi, H. (2025). Coastal flood modelling of Jakarta using the SFINCS, a reduced-physics solver with high computational efficiency. *IOP Conference Series: Earth and Environmental Science*, *1464*(1), 012018. https://doi.org/10.1088/1755-1315/1464/1/012018

Biographies of Authors

Aswin Kurnia Ramadhan, student at the Graduate School of Sustainable Development, Universitas Indonesia. His research background spans spatial analysis applied to energy, environmental, and coastal systems, with current interests in coastal flood risk assessment and climate adaptation planning.

- Email: aswin.kurnia.r@gmail.com
- ORCID: N/A
- Web of Science ResearcherID: N/A
- Scopus Author ID: N/A
- Homepage: N/A

Wezia Berkademi, Lecturer at the Graduate School of Sustainable Development, Universitas Indonesia. Her expertise covers environmental science, environmental economics, and statistical modelling, with research interests in coastal ecosystems and environmental resilience.

- Email: wezia.b@ui.ac.id
- ORCID: N/A
- Web of Science ResearcherID: N/A
- Scopus Author ID: 57222903042
- Homepage: https://sinta.kemdiktisaintek.go.id/authors/profile/6856808

Rachmadhi Purwana, Professor of Public Health at the Graduate School of Sustainable Development, Universitas Indonesia. His research covers environmental health, pollution studies, and disaster-related public health risks in Indonesia.

- Email: rachmadhi@hotmail.com
- ORCID: N/A
- Web of Science ResearcherID: N/A
- Scopus Author ID: 57192905097
- Homepage: https://sinta.kemdiktisaintek.go.id/authors/profile/6657707